Title	Statistical analysis of fuel failures in large break loss-of-coolant accident (LBLOCA) in EPR type nuclear power plant
Author(s)	Arkoma, Asko; Hänninen, Markku; Rantamäki, Karin; Kurki, Joona; Hämäläinen, Anitta
Citation	Nuclear Engineering and Design. Elsevier. Vol. 285 (2015), Pages 1-14
Date	2015
URL	http://dx.doi.org/10.1016/j.nucengdes.2014.12.023
Rights	This post-print version of the article can be downloaded for personal use only.

Statistical analysis of fuel failures in large break loss-of-coolant accident (LB-LOCA) in EPR type nuclear power plant

Asko Arkoma*, Markku Hänninen, Karin Rantamäki, Joona Kurki, Anitta Hämäläinen

VTT Technical Research Centre of Finland, Tietotie 3, P.O. Box 1000, FI-02044 VTT, Finland

*Corresponding author. Tel.: +358 40 825 7010. Fax: +358 20 722 5000. E-mail address: asko.arkoma@vtt.fi

ABSTRACT

In this paper, the number of failing fuel rods in a large break loss-of-coolant accident (LB-LOCA) in EPR-type nuclear power plant is evaluated using statistical methods. For this purpose, a statistical fuel failure analysis procedure has been developed. The developed method utilizes the results of nonparametric statistics, the Wilks' formula in particular, and is based on the selection and variation of parameters that are important in accident conditions. The accident scenario is simulated with the coupled fuel performance – thermal hydraulics code FRAPTRAN-GENFLO using various parameter values and thermal hydraulic and power history boundary conditions between the simulations. The number of global scenarios is 59 (given by the Wilks' formula), and 1000 rods are simulated in each scenario. The boundary conditions are obtained from a new statistical version of the system code APROS. As a result, in the worst global scenario, 1.2% of the simulated rods failed, and it can be concluded that the Finnish safety regulations are hereby met (max. 10% of the rods allowed to fail).

Keywords: loss-of-coolant accident, EPR, Wilks' formula, FRAPTRAN-GENFLO, APROS, statistical fuel failure analysis

1. INTRODUCTION

In safety assessments, the estimation of the fraction of failing rods is traditionally based on conservative analyses but this approach has several downsides. Sometimes it is hard to judge whether the assumptions are conservative because the phenomena in the reactor are highly nonlinear. Additionally, conservative methods often lead to excessive margins and that way to economic losses. The development of statistical fuel failure analysis started worldwide when the U.S.NRC (1988) revised its rules to allow realistic best-estimate methods complemented with uncertainty analysis alongside with the old conservative approach.

Before the current efforts in this field at VTT, there has not been a statistical or any other systematic tool in Finland for the evaluation of the number of failing rods. The Regulatory Guides on nuclear safety (STUK, 2013) set by the Finnish nuclear safety authority STUK introduce a number of design criteria that the fuel has to fulfil in accident conditions[1]. Among others, the following criteria are applicable in LOCA conditions (Class 2 accident):

- less than 10% of the rods in the reactor are allowed to be damaged
- the limit for the peak cladding temperature is 1 200 ºC.

The statistical calculation system has to show that the number of failing rods does not exceed the allowed limit. The development of such a system started at VTT in 2006, and the methodology has been presented in TopFuel conference (Arffman and Rintala, 2011).

The basis of the current analysis is that the fuel performance code which is appropriately modelling the accident behaviour should indicate the fuel rod failure and therefore no additional failing criteria are needed. Thus the essential output from a calculation is the binary information whether the rod fails or not. In addition, the peak cladding temperatures obtained as by-products of the simulations are compared with the temperature limit of 1 200 ºC.

The applied simulation codes are a modified version of the FRAPCON code for the steady-state simulations (U.S.NRC, 2011a) and FRAPTRAN-GENFLO for the transient calculations (Hämäläinen et. al., 2001; U.S.NRC, 2011b). The thermal hydraulics boundary conditions needed for the transient analysis with FRAPTRAN-GENLO are obtained from the system code APROS (www.apros.fi). In addition to transient boundary conditions, the steady-state power histories needed in FRAPCON simulations are generated with neutronics codes.

As the initiating event in the analysed LB-LOCA scenario, a double ended break is opened in a cold leg. Due to pressure decrease, reactor and turbine trips follow. Simultaneously with the turbine trip, the offsite power is lost (LOOP) and the main recirculating coolant pumps start to coast down. Due to loss of coolant, the core is uncovered. The content of the accumulators is injected to the primary loop when the accumulator pressure is reached. After a delay, the diesel generators are started and the medium, and later on the low head safety injections start injections and the core is quenched.

The theoretical basis of the applied method is elaborated in Section 2. The application of the procedure and the simulation tools are presented in Section 3, and the results and discussion in Section 4. Finally the summary is given in Section 5.

2. METHODS FOR STATISTICAL FUEL FAILURE ANALYSES

There are various approaches for a statistical fuel failure analysis. In order to produce a statistically reliable estimation on the number of failing rods, a huge number of simulations are needed. The analysis methods do not exclude each other, and can thus be used in parallel to diminish the amount of required computer code simulations. The constant growth in computer resources has affected, and will continue to affect the choice between various statistical methods.

[1] The criteria are given generally for all postulated accidents. Accidents are further divided to Class 1 and 2 according to their initiating event frequency: $10^{-2} – 10^{-3}$/ year in Class 1, and less than that in Class 2. The criteria are set separately for the two classes.

2.1 Classification of initial parameters and definition of their distributions

The initial parameters of statistical analysis can be divided into two groups by their range. Global parameters have an effect on all the rods in the reactor, whereas local parameters bring variation only to individual rods. For example, the model parameters of a fuel performance code are global, whereas fuel manufacturing parameters are local. The division of parameters into global and local should somehow be taken into account in the analysis because the fuel rods have some correlation with each other. However, the magnitude of the correlation is unknown because it is not precisely known which parameters have the biggest influence on the integrity of the rod during an accident.

As a first step of a statistical analysis, the varied parameters have to be chosen and their distributions defined. The selection may be conducted by means of a sensitivity analysis with fuel modelling codes and by searching specific variation ranges from open literature, but a lot of expert judgment is still needed. Fuel manufacturing parameter ranges are provided by the fuel manufacturer. The choice between various statistical methods can also limit the number of parameters that can be included in the analysis. This is the case if one uses for instance response surfaces for combining the uncertainties. Typically the parameter values are normally distributed around the nominal value, but in some cases other distributions like uniform or triangular distributions are closer to reality and should be preferred.

2.2 Tolerance interval method

The tolerance interval theory (Martin and Nutt, 2011; Panka and Keresztúri, 2007) gives the means to determine the number of simulations that are needed for the statistical analysis when the intended probability content and confidence level are predetermined. This method is adopted as the basis of the procedure developed at VTT.

The teoretical basis of the tolerance interval method was set by Wilks (1941). The starting point of the problem setting is that N sets of initial parameter values are sampled from their corresponding distributions. These sets are used as simulation code inputs, and as a result there will be N values of a result parameter, accordingly. The distribution of the result parameter is an unknown function, here denoted by $f(y)$. With the tolerance interval method, the upper and lower limits in the distribution $f(y)$ are chosen in a way that a given probability content γ would be inside those limits with a confidence level β. This is mathematically expressed as (Panka and Keresztúri, 2007; Guba et al., 2003):

$$P\left(\int_L^U f(y)dy > \gamma\right) = \beta \cdot \qquad (1)$$

Next, a set of result parameter values picked from the unknown distribution $f(y)$ are arranged in ascending order. When the minimum value is marked with index r and the maximum value with index s, Equation (1) can be written:

$$\beta = 1 - \sum_{j=s-r}^{N} \binom{N}{j} \gamma^j (1-\gamma)^{N-j} \cdot \qquad (2)$$

In the case of one-sided tolerance interval, the lower bound L is chosen to be $-\infty$ (r=0) and the upper bound U is the highest value (in first order Wilks') in the random sample picked from the distribution (s=N). Thus, inserting r=0 and s=N into Equation (2), one gets the relation known as the Wilks' formula (in first order and for one-sided tolerance limit):

$$\beta = 1 - \gamma^N \cdot \qquad (3)$$

When this formula is applied to safety evaluations, the generally acceptable level is a 95% probability with a 95% confidence that the number of failed rods would not overstep the allowed limit. When the corresponding values are inserted into Equation (3), thus γ = 0.95 and β = 0.9515, the number of cases comes out as 59. This figure applies when there is only one result parameter but the analysis can be broadened out: if one would like to examine multiple output parameters, more calculations are needed. On the other hand, the number of calculations is independent of the number of initial parameters included in the analysis.

In practice, when using the Wilks' formula, one can state that when all the rods in the reactor are simulated 59 times with variations between each of the 59 scenarios, and if the number of failed rods in the worst case is below the allowed limit, then the safety requirements are rightly met with the probability of 95% and with the confidence level of 95%. As

that kind of number of simulations is out of reach with the computer resources of today, some other method or approach is needed alongside in order to reduce the amount of simulations.

The dispersion of the estimated upper tolerance limit may be reduced by using the Wilks' formula in higher order, i.e. increasing the sample size N (OECD/NEA, 2007, Martin and Nutt, 2011). Then, the n^{th} highest value is taken among the results parameters, and it corresponds to the n^{th} order Wilks'. Limiting the dispersion means that the conservatism is also reduced, and that is especially needed when the upper tolerance limit approaches the regulatory acceptance criterion. However, the numbers of simulations in the second, third and fourth order are 93, 124 and 153, respectively, and in order to save computation time, additional simulations will not be made if not found necessary in fulfilling the acceptance criterion.

2.3 Various approaches for reducing the number of simulations

Various approaches for reducing the number of simulations have been developed. The established methods include for example the use of response surfaces (Panka and Keresztúri, 2007; Technical Program Group, 1989) and grouping of the rods (Hatala, 2005). The lack of statistical accuracy may be compensated by introducing some conservative assumptions.

For the same purpose and in the same way as the response surfaces are used, neural networks may be applied (Pedroni et al., 2010; Montes et al., 2009; Cadini et al., 2008; Santosh et al., 2007; Gozalvez, 2006; Na et al., 2004; Ortiz and Requena, 2004; Faria and Pereira, 2003). Compared to response surfaces, neural networks are a more sophisticated tool for describing nonlinear phenomena. Neural networks are also more flexible because those are less restrictive with respect to the number of initial parameters to be included in the analysis. Naturally, this approach also has its own downsides. Because of the intrinsic characteristics of neural networks, the performance of a network varies between simulation runs even if the training data is the same. As always when operating with neural networks, one has to take extra care when interpreting the results. Network overfitting could become a problem. The same may occur if one uses an insufficient amount of data to train the network in relation to the number of layers and neurons in it. Generally, one can use more complex network structures and get more complicated phenomena into view if a large data set is used for training.

3. APPLICATION OF THE DEVELOPED ANALYSIS PROCEDURE

It is important to take into account the propagation of modelling uncertainties throughout the calculation system. Namely, the boundary conditions of a fuel performance code come from a system code and from a neutronics code, and those have their own uncertainties (OECD/NEA, 2009, 2007; Pourgol-Mohammad, 2009). The uncertainties in the boundary conditions are taken into account by simulating the accident 59 times with the newly introduced statistical version of the system code APROS. Meanwhile, the uncertainties related to the neutronics calculations used to produce the base irradiation pin power histories are left outside the study as only one base irradiation power history is considered for the core. The variation of the core power history and the consequent propagation of the uncertainties to pin power histories may be considered in future studies.

There are thus 59 global variations of the accident with different boundary conditions and different set of model parameter values between each of the variations. Next for each global scenario, a large number of cases with various local parameter values are calculated. The number of calculations is chosen to be 1000 for each global variation. This number is chosen so that the computation time of the simulations still remains reasonable. In order to be able to pinpoint the worst global scenario unambiguously, the same rods are chosen to be simulated in each global scenario. Thus the locations and the local parameter values of the 1000 rods are the same in each global scenario.

The flowchart of the calculation system is presented in Fig. 1. On the grounds of the above mentioned calculations, the worst global case is determined based on the highest number of failed rods. The number of failed rods in the worst global case can then be directly scaled to find out the number of failed rods in the whole reactor. This approach is on the conservative side because with a smaller, but still sufficient, number of cases, the deviation of the number of failures grows. Therefore, the biggest failure number is likely to be higher than it would have been if all the cases had been calculated instead of an extrapolation. Moreover, based on the tolerance interval theory, only the highest number of failed rods counts. In this case, a sufficient number of simulations needs to be calculated in order to limit the deviation due to the extrapolation of the rod failure numbers. The chosen number of simulations (1000) is considered in this case to be enough.

Finally, in order to complete the analysis and make it more thorough, local parameter values are sampled for all the rods in the loading pattern. Then all the rods are simulated with FRAPTRAN-GENFLO using the global parameter

values of the worst global case deduced in the first phase. This is mathematically more justified than the conservative result because now all the simulations required by the Wilks' formula are conducted in the worst global scenario.

Alongside with the second step described above, the same sampled local parameter values for all the rods are used in a neural network analysis. This last phase is done in order to verify the suitability of neural networks for this kind of analysis. For example, if one does not have time or computer resources available to simulate all the rods in a reactor in the second phase, one could apply neural networks for this. Using the 1000 simulations per global scenario, one could train a neural network for each global scenario or just for the worst global scenario, and then use the network(s) to obtain an estimation of the number of failed fuel rods in the whole reactor. In theory, neural network analysis would give a wider margin to the acceptance limit as it is more realistic than the conservative approach. In this paper, one neural network is fitted for the worst global scenario. The neural network analysis is conducted using a MATLAB built-in neural network software package, the Neural Network Toolbox™. It is a general-purpose tool for neural network analyses, and its basic use is quite simple.

3.1 Applied codes and programmes

The primary calculation tool is the coupled fuel performance–thermal hydraulics code FRAPTRAN-GENFLO. FRAPTRAN (version 1.4) is a single-rod fuel performance code developed by PNNL for U.S.NRC and it is designed to model accident conditions specifically (U.S.NRC, 2011b). The general thermal hydraulics code GENFLO has been exclusively developed at VTT (Miettinen and Hämäläinen, 2002). The thermal hydraulics modelling in the stand-alone FRAPTRAN has been found to be unsatisfying, and therefore for years ago, the coupling with an external thermal hydraulics code has been introduced.

For each time-step and axial segment, GENFLO calculates the coolant temperature and the clad-to-coolant heat transfer coefficients. GENFLO is fast-running due to a non-iterative solution of the field equations. It contains a five-equation thermal hydraulics model (two energy and mass equations, one momentum equation) with drift-flux phase separation. A short stabilization phase must be calculated with stand-alone GENFLO prior to the coupled FRAPTRAN-GENFLO calculation. The coupled code has been validated against results from the Halden Project IFA-650 LOCA tests (OECD/NEA, 2010). Recently, the coupled code has been improved in order to be able to simulate the long-lasting reversed core flow which is possible in EPR.

The steady-state initializations of the stacked calculations are performed with the U.S.NRC/PNNL FRAPCON code (version 3.4). An advanced statistical version of FRAPCON developed at VTT is used (Stengård and Kelppe, 2003). It enables the variation of selected model parameters shown in Table 2.

For the FRAPCON simulations, the steady-state power histories of all the rods in the reactor are needed. This data was created using the codes from the CMS family developed by Studsvik Scandpower. SIMULATE 3 (Studsvik Scandpower, 2003) was used to simulate the core and to obtain the desired power histories.

The cladding failure is a FRAPTRAN output. The ballooning model of FRAPTRAN assumes that when the effective plastic strain in any axial segment of the cladding exceeds the instability strain given by the material properties package MATPRO, local non-axisymmetric cladding ballooning begins. The rod is considered to fail when the indicator for the overall rod failure is triggered.

The actual calculation system consists of several small programmes that have been coded for data processing, writing inputs and steering the calculations. Some external programmes are also used, like the sampler module of the software tool SUSA, Software system for Uncertainty and Sensitivity Analysis, developed by the German research organisation GRS (Kloos, 2008). SUSA is here utilized for generating random parameter values from specified distributions.

A Perl script has been written to steer the stacked FRAPTRAN-GENFLO calculations on a Linux cluster. Major changes to the FRAPTRAN and GENFLO codes for the purpose of the statistical analysis were avoided. Most of the output files of FRAPTRAN and GENFLO are unnecessary when conducting the analysis and are therefore suppressed or strongly reduced.

In order to obtain the time-dependent boundary conditions for the fuel performance code calculations, the overall progress of the accident is simulated with the system code APROS. The APROS code is developed and maintained jointly by VTT and Fortum. The relevant boundary conditions obtained from APROS are the enthalpy and the mass

flows of both liquid and vapour at the channel inlet and outlet, the coolant pressure and the rod power including the axial power profiles.

The applied dynamic one-dimensional two-phase flow model of APROS simulates the behavior of a system containing gas and liquid phases. The system is governed by six partial differential equations, from which pressures, void fractions and phase velocities and enthalpies are solved. The phases are coupled to each other with empirical friction and heat transfer terms, and those strongly affect the solution. The governing equations are discretized with respect to time and space and the resulting linear equation groups are solved by the equation solving system of APROS. The heat transfer model of APROS includes all heat transfer modes from single phase heat transfer to the simulation of the boiling crisis and re-flooding of the over-heated rods (Hänninen, 2009).

3.2 Varied parameters and their distributions

The parameters chosen to be varied in the VTT's system are collected into Tables 1 (APROS) and 2 (FRAPCON, FRAPTRAN-GENFLO). The main idea in the performed statistical analysis is that the parameters that are important regarding the whole core are varied in APROS, and the parameters that are important in fuel behaviour analysis are varied in fuel performance codes. Therefore, the same parameters are not varied in APROS and FRAPCON / FRAPTRAN-GENFLO. Instead, the significance of a parameter is assessed in each code, and the parameter is varied in the code in which it has a stronger impact.

The goal is to make the statistical analysis in a realistic best-estimate manner as opposite to a conservative analysis. Therefore a normal distribution is used for most of the parameters since that is more realistic than a uniform distribution. In the APROS simulations, a normal distribution has been assumed for each parameter. The 12 global parameters and their ranges used in the APROS analyses are based mainly on the BEMUSE data (OECD/NEA, 2009, 2007) but also other publically available data has been used (Freixa, 2011, 2010).

The global variation is taken into account by model parameter variations in FRAPCON and GENFLO, and by using various linear power histories and thermal hydraulic boundary conditions (both from APROS) in each global scenario. No model parameters are varied in FRAPTRAN as there is no statistical version of FRAPTRAN available at the moment. The steady-state and transient power histories have not been varied for example by multiplying with a random sampled constant factor. This is justified by the fact that firstly, there is natural variation of steady-state power when the simulated rods are random sampled from the loading pattern, and secondly, different transient power histories are applied in each global scenario.

The varied model parameters and their ranges in FRAPCON and GENFLO are based on previous analyses made at VTT. Adding more parameters to be varied in the statistical version of FRAPCON is a matter to be addressed in the future. Generally, the parameters affecting the thermal hydraulics are varied in the system code APROS. However, the parameters now varied in GENFLO cannot be currently varied in APROS and therefore those are taken into consideration in GENFLO. Meanwhile, fuel-related parameters are kept at their best-estimate values in the system code and varied only in the fuel performance codes.

3.3 Sampling of rods to be analysed

In the simulated scenario, the accident occurs after cycle 4. Cycle 4 is the first cycle that can be considered as an equilibrium cycle. In addition to various power histories, there are many ^{235}U enrichments, and gadolinium rods with various Gd contents. The cladding material is M5™ (www.epr-reactor.co.uk).

At the end of cycle 4, there are five different assembly types in the core. These types vary in ^{235}U enrichment, the number of Gd rods in the assembly, and the Gd_2O_3 content in the Gd rods. About half of the assemblies have been in the core only for the cycle 4 while the rest have been irradiated for two cycles. All but one of these assemblies have been in the core for cycles 3 and 4. However, one assembly was removed from the core after the first cycle and reinserted to the core for cycle 4, i.e. it was out of the core during the cycles 2 and 3. Consequently, at the end of cycle 4, there are no assemblies from cycle 2. The cycle lengths for cycles 1, 3 and 4 were 18, 24 and 24 months, respectively.

The total number of rods in the reactor is 63 865, and the number of Gd rods is 5 356. The 1000 rods are sampled among all the bundles and all the possible rod positions. If there is a guide tube in the sampled position, or the same rod is sampled anew, a new location is chosen.

3.4 APROS boundary conditions for FRAPTRAN-GENFLO

In APROS, the reactor core is divided into 20 axial nodes for the solution of thermal hydraulics and neutronics. The core is divided into 17 thermal hydraulic channels. The locations of the thermal hydraulic channels related to the fuel bundles are presented in Fig. 2. As the EPR core is open, i.e. there are no shrouds around the fuel assemblies, there are cross flows in the core. The cross flows are important to be taken into account in the simulations as those balance the flows between bundles with various power levels. However, a single FRAPTRAN-GENFLO simulation is made for a closed subchannel, and the cross flows cannot be explicitly taken into account. Now, as the core is divided in APROS into thermal hydraulic channels consisting of several bundles instead of only one bundle per channel, the cross flows are being taken into account in the boundary conditions that APROS produces for FRAPTRAN-GENFLO. Thus, the cross flows are considered in FRAPTRAN-GENFLO simulations implicitly via boundary conditions from APROS.

In the APROS output files, the transient begins right after 0 s. In a FRAPTRAN-GENFLO analysis, a short steady-state with the coupled code is simulated prior to the accident, and therefore a 10-second steady-state is added to the power history and to the thermal hydraulic boundary conditions. The FRAPTRAN-GENFLO simulations are continued up to 700 seconds.

The linear power histories and thermal hydraulic boundary conditions are available for 17 channels except the inlet enthalpy for liquid and vapour which are given for eight sectors. The eight enthalpy sectors take into account the asymmetric temperature distribution in the core resulting from the break in one of the cold legs. The axial power profiles are available for all the 241 bundles. The same static beginning-of-transient axial power profiles are used in all the 59 global scenarios. The linear power histories available for the channels are further refined for each bundle by defining a multiplier from an APROS output file. Thus, the total number of linear power histories applied in the simulations is 59 × 241 = 14 219, the total number of axial power profiles is 241, and the total number of thermal hydraulic boundary conditions is 59 × 17 = 1 003. These boundary conditions are used for the single rod simulations with no further refining to pin level.

The variation of power between the global scenarios is small. The variation of decay heat power is larger between the coolant channels than between the global scenarios. To illustrate the power histories used in FRAPTRAN-GENFLO simulations for the sampled rods, the power histories in global scenario 47 are plotted in Fig. 3. One can see that there are various initial power levels in the rods, ranging from <~3 to >~30 kW/m. Also the decay heat power after the scram is shown in the figure. The curves corresponding to the rods that failed in this scenario are indicated with markers.

The thermal hydraulics boundary conditions are filtered in order to make the simulations converge more easily. The filtering is started when 20 seconds has passed in the APROS boundary conditions, and it is done for all the thermal hydraulic boundary conditions coming from APROS. Meanwhile, the transient power is not filtered. A simple exponential smoothing is used for the filtering (Brown and Meyer, 1961):

$$x_t = \alpha s_t + (1-\alpha) x_{t-1}. \qquad (4)$$

Here the new filtered value x_t is the weighted average of the current value s_t and the filtered value x_{t-1} from the previous time-step. The smoothing factor α is now given a value 0.4. An example of the filtering is given in Fig. 4 where the filtered and non-filtered water flows at channel inlet are presented. The highest peaks are reduced but this has negligible influence on the calculated results, e.g. cladding temperatures.

3.5 Duration of the simulations

Statistical analysis unavoidably takes a lot of time. Statistical version of FRAPCON is fast-running but the transient calculations are slower to conduct. The duration of a single FRAPTRAN-GENFLO calculation depends among other things on the time-step.

Various time-step sizes were tested in order to find a balance between the computation time and reaching the convergence. With the coupled code, shorter time-steps are usually required than with the stand-alone FRAPTRAN due to numerical reasons. Consequently, a time-step of 5.0 ms was used throughout the transient, and with this choice most of the simulations were successful. With 32 simultaneous transient simulation on a Linux cluster, the 59 000 simulations took in real time 12 days 5h 43 min.

4. RESULTS AND DISCUSSION

In the following, the number of failing fuel rods in each global scenario is presented. Also the cladding maximum temperatures and hoop strains are given. As described in Section 3 and presented in Fig. 1, the number of failing fuel rods is achieved in three ways: by a conservative approach consisting of 1000 simulations per global scenario, by simulations of all the rods in the reactor in the worst global scenario, and finally, by performing a neural network analysis. First, the main findings of the APROS analysis are briefly presented.

4.1 APROS results

The highest maximum cladding temperature in the APROS calculations was achieved in thermal hydraulic channel 4 (see Fig. 2) when the input values of global scenario 3, given in Table 3, were used. The cladding temperature evolutions in channel 4 are given in Fig. 5 for all the 59 scenarios. Six additional curves are also plotted in Fig. 5. The lowest and the highest maximum temperatures at each point in time among the 59 scenarios in channel 4 are presented, as well as the median and average temperatures at each point in time. Two extra simulations are conducted using the nominal, i.e. best-estimate, and conservative input values given in Table 1. Based on the results presented in Fig. 5, it can be stated that the requirement concerning the peak cladding temperature is met as the highest calculated temperatures are well below 1 200 ºC.

A clear reason why certain combination of input parameter values gave high and low extreme values could not be found. The anticipated conservative case in which conservative input values were chosen based on engineering judgement did not lead to the absolute highest cladding temperatures, see Fig. 5. In general, it was very difficult to predict prior to the simulations by plain engineering judgement which combination of the varied input parameters would give the worst results with respect to the maximum cladding temperature. However, the use of the conservative input values delayed the final quenching and in that respect the chosen input values were conservative.

4.2 Simulation of 59 global scenarios with 1000 cases in each

From the total of 59 000 simulations, the number of simulations that ended up with a rod failure was 142. It should be noted that the same 1000 rods were simulated in each global scenario, and in many cases, the same rod failed in various global scenarios. The numbers of rods that failed in each global scenario are shown in Fig. 6. As can be seen from Fig. 6, the number of failing fuel rods was the highest in global scenario 47, 12 rods. Thus in the worst case, 1.2% of the rods failed.

Based on the simulations made, it is not possible to say whether the highest number of failing rods results from the APROS boundary conditions or from the sampled global parameters; it would require further analysis. The global parameter values in scenario 47 are presented in Table 4. When analysing the failed cases, it is seen that the fuel failures are more likely to occur in some bundles than in others. This is quite natural as the base irradiation histories and other conditions have similarities for rods within a given bundle.

As mentioned in Section 2, when using the first order Wilks' formula, i.e. the number of global scenarios being 59, the highest value obtained is conservative due to dispersion. In this case, the highest value, 1.2%, is far below the acceptance criterion, 10 %, and thus it can be concluded that using the Wilks' formula in higher order for reducing the conservatism is not necessary.

As an example, the axially maximum cladding outer surface temperatures in global scenario 47 are plotted in Fig. 7. The curves corresponding to the rods that failed in this scenario are indicated with markers. In each global scenario, the highest peak cladding temperatures emerge soon after the beginning of the accident, and are at the same level in all the global variations, around 900 ºC. Slightly higher peak temperatures compared to the other global scenarios are found in scenarios 12, 19, 43 and 49. The cladding temperatures do not drop off at all for some simulated rods; this behaviour is

typical with extreme values of the drift-flux model parameters of GENFLO. Finally, it can be said that like the APROS results, also the FRAPTRAN-GENFLO analysis shows that the requirement concerning the limiting peak cladding temperature, 1 200 ºC, is met.

Compared to the APROS results, the maximum cladding temperatures in FRAPTRAN-GENFLO simulations were higher and the highest values were obtained clearly earlier in transient than those obtained with APROS, cf. Figs. 5 and 7. Note that the transient starts at 10 s in FRAPTRAN-GENFLO simulations due to the added steady-state period whereas in APROS plot, the starting time is at 0 s. Much of the differences in the maximum temperatures between the APROS and FRAPTRAN-GENFLO results can be explained by the differences in the handling of the fuel-cladding gas gap conductance. In APROS, a constant value of 10 000 $W/m^2/K$ is used, whereas in FRAPTRAN, the gap conductance is calculated axially and with time, and it is thus more realistic.

The highest calculated total hoop strains are over 8% (in global scenarios 1, 9, 12 and 47), and all the rods that have strains over this fail. The total hoop strains consist mainly on plastic strains. The highest total and plastic strains are 8.8% and 8.4%, respectively, both in global scenario 9. The lowest total hoop strain in a failed rod is ~5.6% (in several global scenarios). From the results it can be deduced that if there are rod failures in a global scenario, the strains in the failed rods are at the upper end of the strain scale of this study. The total hoop strains in the global scenario 47 are plotted in Fig. 8. Again, the curves corresponding to the failed rods are indicated with markers.

Some of the simulations crashed because of FRAPTRAN or GENFLO errors. When the simulation failed because of FRAPTRAN, it happened right at the start of the calculation in all the cases except one. The erroneous simulations occurred with the same 4 or 5 rods in all the global scenarios. The reason for the simulation failure was not further studied but it can be speculated to be related to the sampled input values.

The GENFLO errors resulted from a failure in the mixture mass calculations. Reducing the time-step did not help reaching a convergence but with an increased time-step of 10.0 ms, however, the number of GENFLO errors dramatically decreased. Therefore, all the simulations that ended up with a GENFLO error were re-calculated with a larger time-step. Consequently, most of the GENFLO errors disappeared. The change in time-step did not affect the number of failing rods nor the FRAPTRAN errors. The rods of the erroneous simulations were located in five different coolant channels and in various bundles. The highest number of crashed simulations (57) due to GENFLO was in global scenario 3.

4.3 Simulation of all the rods in the reactor in the worst global scenario

Using the boundary conditions and the global parameter values of the worst global scenario (in terms of the number of failed rods), all the 63 865 rods in the loading pattern were simulated with FRAPTRAN-GENFLO. As a results, in scenario 47, the total number of failed rods was 517, and the number of survived rods was 63 068. None of the simulations ended with a GENFLO error. This was also the case with the 1000 simulations performed in the first phase of the analysis in scenario 47. The number of simulations that ended with a FRAPTRAN error message was 280 which is 0.44% of all the calculations. The percentage of failed rods to all calculations is 0.81%, a figure which is lower than the one gained in the first phase, 1.2%. This is expected, as when the number of simulations in a global scenario is increased, the dispersion in the estimation decreases, and thus the result is less conservative.

The axially maximum cladding outer surface temperatures are plotted in Fig. 9. It can be seen that the highest cladding temperatures are at the same level as in the first 1000 simulations, cf. Fig. 7. Also the total hoop strains in Fig. 10 show similar behaviour than the ones plotted in Fig. 8. However, there are five rods in which the strain is simulated to be significantly higher than what is seen in Fig. 8. The hoop strains of those rods are clearly above the two groups of strains located around 6% and 8% in Figs. 8 and 10. Thus, the first 1000 simulations could not catch the highest failure strains. The highest failure strain is about 12.5%.

4.4 Neural network analysis

The applied network type is a feed-forward backpropagation network. There are a number of training functions included in the Neural Network Toolbox™ but here the default function is used. The function utilizes the Levenberg-Marquardt algorithm for training.

In this work, the input data of the neural network analysis consists of the sampled parameter values for the 1000 rods in global scenario 47, and the corresponding simulation results of rod failure / non-failure. The input data in neural network analysis is usually divided into three sets: training, validation and test set. The first set is used for teaching the network, and the second is used to stop the teaching when the mean squared error in the validation set turns into a

growing trend which is a sign of overfitting. The last set is used as an independent data for testing the trained network. The fraction of data for each set is chosen by the user; the default fractions are 70%, 15% and 15%. Now, as there are only 12 failed rods in the worst global scenario, the test set is not used in order to have more data for teaching the network. Consequently, the fractions 85%, 15% and 0% for the three sets are used instead. Testing the network is done when the network is applied in the subsequent analysis covering all the rods in the reactor. After training, the performance of a network is evaluated with the regression constant values as presented in Fig. 11 for a network used here as an example.

If the sampled parameter values would be the only input to the neural network, the various base irradiation histories and transient power histories of the rods would not be taken into account. Therefore, the rod burnup and the initial power prior to the transient have been included to the teaching data. The latter may be justified by the fact that when the transient power histories of the 1000 rods are normalised to start from unity, the curves coincide, which means that a single value (e.g. initial transient power) may be applied to illustrate a transient power history.

When teaching and applying the network, the cases that were crashed due to FRAPTRAN errors were removed from the data. In the application phase, the 1000 rods used for teaching and validating the network were not used as an input to the network.

Various network configurations were tested (for example consisting of two hidden layers) but the default structure in MATLAB was eventually used, consisting of one hidden layer with ten neurons in it. This configuration was adopted because no clear difference in predictive capabilities was found between the tested configurations.

The target of the network is a binary number, 0 for survival and 1 for a failure, but the output from the network is a value from a continuous distribution between 0 and 1, and slightly beyond these. Therefore, a criterion for the rod failure has to be defined, i.e. how close to unity must the network output value be in order to conclude that the rod is predicted to fail. In the performed analysis, various criteria were tested and the number of the failing rods varied accordingly. This is seen in Fig. 12 where the predicted failure numbers obtained from a trained network used here as an example are presented. By comparing the y-axis range in Fig. 12 to the number of simulated rod failures, it can be stated that with this network the number of failing rods is in the same range as in the real simulations. Namely, the number of the simulated rod failures was 505 as the total number of failures among all the rods was 517, and the 12 rods that failed in the set of 1000 rods used for teaching and validation were not used in testing the network. Thus, a neural network could presumably be used instead of fuel performance code calculations if one does not need to know the number of failing rods exactly but just needs to check whether the criterion of 10% of failing rods is met.

To further compare the network results with the simulation results, two histograms are produced. First, the FRAPTRAN-GENFLO results of all the rods in the reactor are organized in a row vector consisting of binary numbers. Then, for the first histogram depicting the survived rods, the indices of the survived rods are searched from the row vector, and the neural network outputs that correspond to these indices are plotted. The data is split into 200 bins. An example of such a histogram is given in Fig. 13. The shape of the histogram varies only a little when the network is re-trained. There are high peaks around zero which means that the survived rods are most often well predicted by the network compared to the simulation results. Note that small peaks are shown also around unity as a sign of incorrect predictions.

The second histogram, depicting the failed rods, is constructed in the same fashion. An example is presented in Fig. 14. The shape of this histogram varies significantly when the network is re-trained. This can be understood by the fact that the number of failing rods used in teaching the network is very limited, only 12. The number of incorrect predictions is high as seen from the high peaks around zero in Fig. 14. In these occurrences the rods are predicted by the network to survive even if in FRAPTRAN-GENFLO simulations those rods are failed. However, there are another set of high peaks around unity, which tells that the network can predict a substantial number of failed rods correctly in spite of the low number of failed rods used for teaching the network.

5. SUMMARY

Using a calculation system for statistical fuel failure analysis, the number of failed fuel rods in LB-LOCA in an EPR was estimated. The number of failing fuel rods in 59 simulated global scenarios ranged from 0 to 12 rods per 1000 simulations. Thus, in the worst case, 1.2% of the simulated rods failed. It can be concluded that according to the statistical analysis performed, the requirement that less than 10% of the rods may fail in a LB-LOCA is met.

Some of the simulations crashed; in the worst global scenario, the percentage of crashed simulations was 0.4%, and the highest percentage among all the scenarios was 6.1%. Even if all the crashed simulations were conservatively considered to stand for a rod failure, the requirement is met. The limitation of the current study is that no model

parameters are varied in FRAPTRAN, and for that, a statistical version of FRAPTRAN should be developed in the future.

The highest peak cladding temperature occurred always soon after the beginning of the accident in FRAPTRAN-GENFLO simulations, and was at the same level in all global variations, around 900 ºC. The requirement concerning the highest peak cladding temperature, 1 200 ºC, is thus met. The highest total and plastic strains were 8.8% and 8.4%, respectively. The lowest total hoop strain in a failed rod was ~5.6%.

Using the boundary conditions and global parameter values of the worst global scenario (in terms of the number of failed rods), all the 63 865 rods in the loading pattern were simulated with FRAPTRAN-GENFLO. The total number of failed rods was in this case 517, corresponding to 0.81% of all the simulated rods. This percentage is lower than the one produced in the first phase, 1.2%, confirming that the result gained in the first phase is conservative.

Preliminary testing of neural networks was done. A neural network is thought to replace the second phase of the analysis, the simulation of all the rods in the worst global scenario. With the trained networks, the number of failing rods is in the same range as in the real simulations but the result is not very accurate. Therefore neural networks may only be used for a cursory glance at the number of failing rods in the reactor scale if the time or resources are short for a more complete analysis.

ACKNOWLEDGEMENTS
The work presented in this paper has been done for the Finnish nuclear safety authority STUK. The statistical procedure has been developed under the auspices of the Finnish Research Programmes on Nuclear Power Plant Safety – SAFIR2010 and SAFIR2014.

CAPTIONS

FIGURES

Fig. 1. Flowchart of the calculation system.

Fig. 2. The reactor core is divided into 17 thermal hydraulic channels in APROS, and the locations of these channels related to fuel bundles are presented here.

Fig. 3. Linear power histories of the 1000 rods in the global scenario 47.

Fig. 4. Thermal hydraulic boundary conditions from APROS are filtered for the FRAPTRAN-GENFLO analyses. The filtering of water flow at channel inlet is given as an example in the figure.

Fig. 5. Maximum cladding temperatures in thermal hydraulic channel 4 in APROS simulations.

Fig. 6. The numbers of the failed fuel rods among the 1000 rods simulated in each of the 59 global scenarios.

Fig. 7. Axial maximum cladding outer surface temperatures of the 1000 rods in the global scenario 47.

Fig. 8. Axial maximum total hoop strains of the 1000 rods in the global scenario 47.

Fig. 9. Axial maximum cladding outer surface temperatures of all the rods in the reactor in global scenario 47.

Fig. 10. Axial maximum total hoop strains of all the rods in the reactor in global scenario 47.

Fig. 11. Linear regression of network targets, i.e. FRAPTRAN-GENFLO results of rod failure / non-failure, relative to the network output.

Fig. 12. The criterion of how close the network output has to be to unity (= designating rod failure) affects the number of failing rods given by a neural network. The x-axis value is the criterion over which the neural network output has to be in order to consider the rod to be failed.

Fig. 13. Neural network predictions for the rods that were shown to survive in the FRAPTRAN-GENFLO simulations. All the rods in the reactor were considered except the 1000 that were used for the training and validation of the network.

Fig. 14. Neural network predictions for the rods that were shown to fail in the FRAPTRAN-GENFLO simulations. All the rods in the reactor were considered except the 1000 that were used for the training and validation of the network.

TABLES

Table 1. Varied input parameters and their ranges in APROS calculations.

Table 2. Varied parameters in FRAPCON and FRAPTRAN-GENFLO simulations. The values and the distributions of fuel manufacturing parameters are confidential.

Table 3. Worst case parameters in APROS simulations leading to the highest maximum cladding temperatures.

Table 4. Global parameter values in global scenario 47 in which the number of failing fuel rods was the highest.

REFERENCES

Arffman, A. (currently Arkoma, A.), Rintala, J., 2011. Statistical Analysis Of Fuel Failures In Accident Conditions. Water Reactor Fuel Performance Meeting, Chengdu, China, paper T3-028

Brown, R. G., Meyer, R. F., 1961. The fundamental theory of exponential smoothing. Operations Research, Vol. 9, No. 5, p. 673-685

Cadini, F. et al., 2008. A model based on bootstrapped neural networks for computing the maximum fuel cladding temperature in an Rbmk-1500 nuclear reactor accident. Nuclear Engineering and Design, Vol. 238, Issue 9, pp. 2165-2172

Faria, E. F., Pereira, C., 2003. Nuclear fuel loading pattern optimization using a neural network. Annals of Nuclear Energy, Vol. 30, Issue 5, pp. 601-613

Freixa, J. et al., 2011. Post-test thermal-hydraulic analysis of two intermediate LOCA tests at the ROSA facility including uncertainty evaluation. The 14th International Topical Meeting on Nuclear Reactor Thermalhydraulics, NURETH-14, Toronto, Ontario, Canada, September 25-30, 2011

Freixa, J. et al., 2010. Thermal-Hydraulic Analysis of an Intermediate LOCA Test at the ROSA facility including Uncertainty Evaluation. The 8th International Topical Meeting on Nuclear Thermal-Hydraulics, Operation and Safety (NUTHOS-8) paper N8P0242, Shanghai, China, October 10-14, 2010

Gozalvez, J. M., 2006. Sensitivity study on determining an efficient set of fuel assembly parameters in training data for designing of neural networks in hybrid generic algorithms. Annals of Nuclear Energy, Vol. 33, Issue 5, pp. 457-465

Guba, A., et al., 2003. Statistical aspects of best estimate method – I. Reliability Engineering and System Safety, Vol. 80, Issue 3, pp. 217-232

Hatala, B., 2005. Quantification of fuel rod cladding failure during LOCA accident. 6th International Conference on WWER Fuel Performance, Modelling and Experimental Support, Albena, Bulgaria

Hämäläinen, A. et. al., 2001. Coupled Code FRAPTRAN – GENFLO for Analysing Fuel Behaviour During PWR and BWR Transients and Accidents. Proceeding of a Technical Committee meeting, IAEA-TECDOC-1320, Halden, Norway

Hänninen M., 2009. Phenomenological extensions to APROS six-equation model. Non-condensable gas, supercritical pressure, improved CCFL and reduced numerical diffusion for scalar transport calculation. VTT Publications 720, ISBN 978-951-38-7367-7

Kloos, M., 2008. SUSA Version 3.6, User's Guide and Tutorial, Software for Uncertainty and Sensitivity Analyses. Gesellschaft für Anlagenund Reaktorsicherheit (GRS) mbH

Martin, R. P., Nutt, W. T., 2011. Perspectives on the application of order statistics in best-estimate plus uncertainty nuclear safety analysis. Nuclear Engineering and Design, Vol. 241, Issue 1, pp. 274-284

Miettinen, J., Hämäläinen, A., 2002. GENFLO - A General Thermal Hydraulic Solution for Accident Simulation. VTT Research Notes 2163, ISBN 951-38-6083-3, ISSN 1455-0865

Montes J. L. et al., 2009. Local power peaking factor estimation in nuclear fuel by artificial neural networks. Annals of Nuclear Energy, Vol. 36, Issue 1, pp. 121-130

Na, M. G. et. al., 2004. Estimation of break location and size for loss of coolant accidents using neural networks. Nuclear Engineering and Design, Vol. 232, Issue 3, pp. 289-300

OECD/NEA, 2010. Benchmark Calculations on Halden IFA-650 LOCA Test Results. NEA/CSNI/R(2010)6

OECD/NEA, 2009. BEMUSE Phase V Report, Uncertainty and Sensitivity Analysis of a LB-LOCA in ZION Nuclear Power Plant. NEA/CSNI/R(2009)13

OECD/NEA, 2007. BEMUSE Phase III Report, Uncertainty and Sensitivity Analysis of the LOFT L2-5 Test. NEA/CSNI/R(2007)4

Ortiz J. J., Requena, I., 2004. Using a multi-state recurrent neural network to optimize loading patterns in BWRs. Annals of Nuclear Energy, Vol. 31, Issue 7, pp. 789-803

Panka, I., Keresztúri, A., 2007. Uncertainty analyses of hot channel calculations – Determination of the number of failed fuel rods. Progress in Nuclear Energy, Vol. 49, Issue 7, pp. 534-545

Pedroni, N. et al., 2010. Comparison of bootstrapped artificial neural networks and quadratic response surfaces for the estimation of the functional failure probability of a thermal-hydraulic passive system. Reliability Engineering and System Safety, Vol. 95, Issue 4, pp. 386-395

Pourgol-Mohammad, M., 2009. Thermal-hydraulics system codes uncertainty assessment: A review of the methodologies. Annals of Nuclear Energy, Vol. 36, Issues 11-12, pp. 1774-1786

Santosh, T.V. et al., 2007. Application of artificial neural networks to nuclear power plant transient diagnosis. Reliability Engineering and System Safety, Vol. 92, Issue 10, pp. 1468-1472

Secchi, P. et al., 2008. Quantifying uncertainties in the estimation of safety parameters by using bootstrapped artificial neural networks. Annals of Nuclear Energy, Vol. 35, Issue 12, pp. 2338-2350

Stengård, J.-O., Kelppe, S., 2003. Probabilistic Version of the FRAPCON-3 Fuel Behaviour Code. VTT Project Report PRO1/T7048/02

Studsvik Scandpower Inc., 2003. SIMULATE-3, Advanced Three-Dimensional Two-Group Reactor Analysis Code, SIMULATE-3 User's Manual. Studsvik Scandpower Report SSP-01/414 Rev 3

STUK - Radiation and Nuclear Safety Authority, Finland, 2013. Regulatory Guides on nuclear safety, chapter B.4.

Technical Program Group, 1989. Quantifying reactor safety margins; Application of Code Scaling, Applicability, and Uncertainty Evaluation Methodology to a Large-Break, Loss-of-Coolant Accident. NUREG/CR-5249

U.S.NRC, 2011a. FRAPCON-3.4: A Computer Code for the Calculation of Steady-State Thermal-Mechanical Behavior of Oxide Fuel Rods for High Burnup. NUREG/CR-7022, Vol. 1, PNNL-19418, Vol. 1

U.S.NRC, 2011b. FRAPTRAN: A Computer Code for the Transient Analysis of Oxide Fuel Rods", NUREG/CR-7023, Vol. 1, PNNL-19400, Vol. 1

U.S.NRC Regulations, Title 10, Part 50, 1988. Domestic Licensing of Production and Utilization Facilities; § 50.46 Acceptance criteria for emergency core cooling system for light-water nuclear power reactors.

Wilks, S.S., 1941. Determination of Sample Sizes for Setting Tolerance Limits. The Annals of Mathematical Statistics, Vol. 12, No. 1, pp. 91-96

www.apros.fi (visited 30.7.2014)

www.epr-reactor.co.uk/ssmod/liblocal/docs/V3/Volume%201%20-%20Overview/1.A%20-%20EPR%20Design%20Description/1.A%20-%20EPR%20Design%20Description%20-%20v3.pdf (visited 9.12.2014)

Table 1

Parameter	*Nominal*	*Min*	*Max*	*Conservative*
Containment pressure [MPa]	0.250	0.200	0.300	0.200
Pump1 inertia [kgm^2]	5210.0	5157.9	55262.1	5157.9
Pump2,3,4 inertia [kgm^2]	5210.0	5105.8	5314.2	5105.8
Decay heat of normal [%]	100.0	92.0	108.0	108.0
Accu2,3,4 pressure [MPa]	4.9800	4.7800	5.1800	4.7800
Accu2,3,4 level [m]	4.4600	4.3600	4.5600	4.3600
Emergency water temperature [°C]	50.00	10.00	50.00	50.00
Emergency water flow [%]	100.00	95.00	105.00	95.00
CCFL parameter	1.0000	0.6900	1.0350	0.6900
Discharge coefficient, RPV side	0.8750	0.7500	1.0000	1.0000
Discharge coefficient, pump side	0.8750	0.7500	1.0000	1.0000
Upper plenum temperature [°C]	336.0	331.00	341.00	341.00

		Distribution $N(\mu,\sigma^2)$ or triangular (mode)	*Min*	*Max*
Global parameters				
FRAPCON	Swelling parameter	normal(1.0; 0.000144)	not defined	
	Creep rate parameter	normal(1.0; 0.25)	0.6	1.1
	Fission gas parameter	normal(0.0; 0.25)	-1	1
	Thermal conductivity parameter	normal(1.0; 0.01)	not defined	
	Cladding corrosion parameter	normal(1.0; 0.0004)	0.6	1.4
GENFLO	Basic drift flux velocity	triangular (1.2)	1.13	1.2
	Drift flux separation constant	triangular (1.1)	1.1	1.2
	Interphasial heat transfer tuning factor	triangular (0.3)	0.1	0.33
	Film boiling heat transfer tuning factor	triangular (0.2)	0.08	0.22
	Transition boiling heat transfer tuning factor	triangular (0.2)	0.18	0.22
Local parameters				
	Cladding inner diameter	normal		
	Fuel pellet diameter	normal		
	Cladding wall thickness	normal		
	Cold plenum length	normal		
	Fuel pellet density	normal		
	Bottom plenum volume	normal		
	Internal fill pressure	normal		

Table 3

Parameter	*Worst case value*
Containment pressure [MPa]	0.2617
Pump1 inertia [kgm^2]	5204.8
Pump2,3,4 inertia [kgm^2]	5176.3
Decay heat of normal [%]	102.29
Accu2,3,4 pressure [MPa]	4.8646
Accu2,3,4 level [m]	4.4915
Emergency water temperature [°C]	38.00
Emergency water flow [%]	102.62
CCFL parameter	0.8844
Discharge coefficient, RPV side	0.88900
Discharge coefficient, pump side	0.90557
Upper plenum temperature [°C]	336.7

Table 4

Parameter	*Value*
Fission gas parameter	0.363080
Thermal conductivity parameter	1.015300
Swelling parameter	0.995770
Creep rate parameter	0.881100
Cladding corrosion parameter	1.016000
Basic drift flux velocity	1.154200
Drift flux separation constant	1.122200
Interphasial heat transfer tuning factor	0.183950
Film boiling heat transfer tuning factor	0.187390
Transition boiling heat transfer tuning factor	0.192250

Figure 1

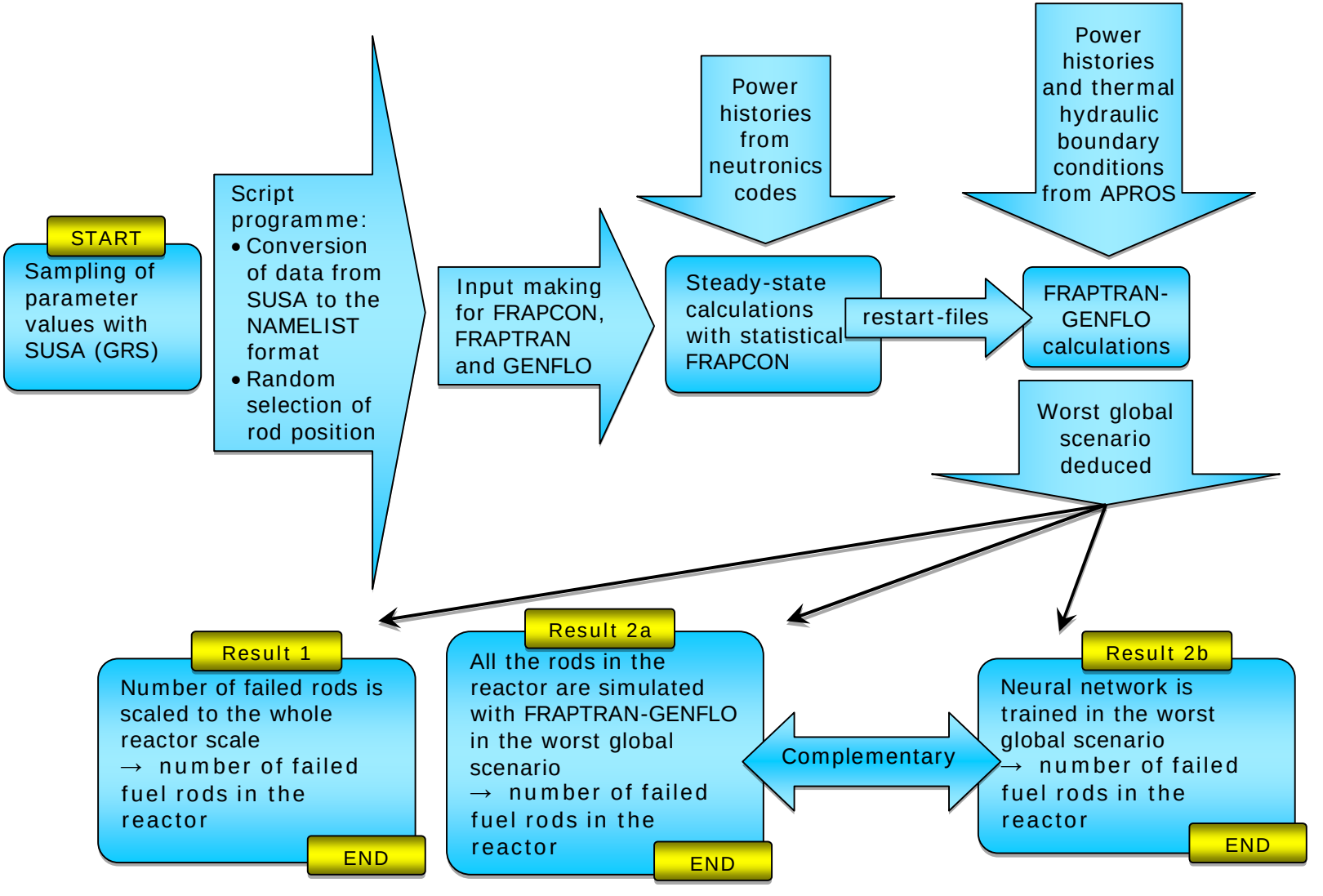
START
Sampling of parameter values with SUSA (GRS)
Script programme:
• Conversion of data from SUSA to the NAMELIST format
• Random selection of rod position
Input making for FRAPCON, FRAPTRAN and GENFLO
Power histories from neutronics codes
Power histories and thermal hydraulic boundary conditions from APROS
Steady-state calculations with statistical FRAPCON
restart-files
FRAPTRAN-GENFLO calculations
Worst global scenario deduced
Result 1
Number of failed rods is scaled to the whole reactor scale
→ number of failed fuel rods in the reactor
END
Result 2a
All the rods in the reactor are simulated with FRAPTRAN-GENFLO in the worst global scenario
→ number of failed fuel rods in the reactor
END
Complementary
Result 2b
Neural network is trained in the worst global scenario
→ number of failed fuel rods in the reactor
END

Figure 2

Click here to download high resolution image

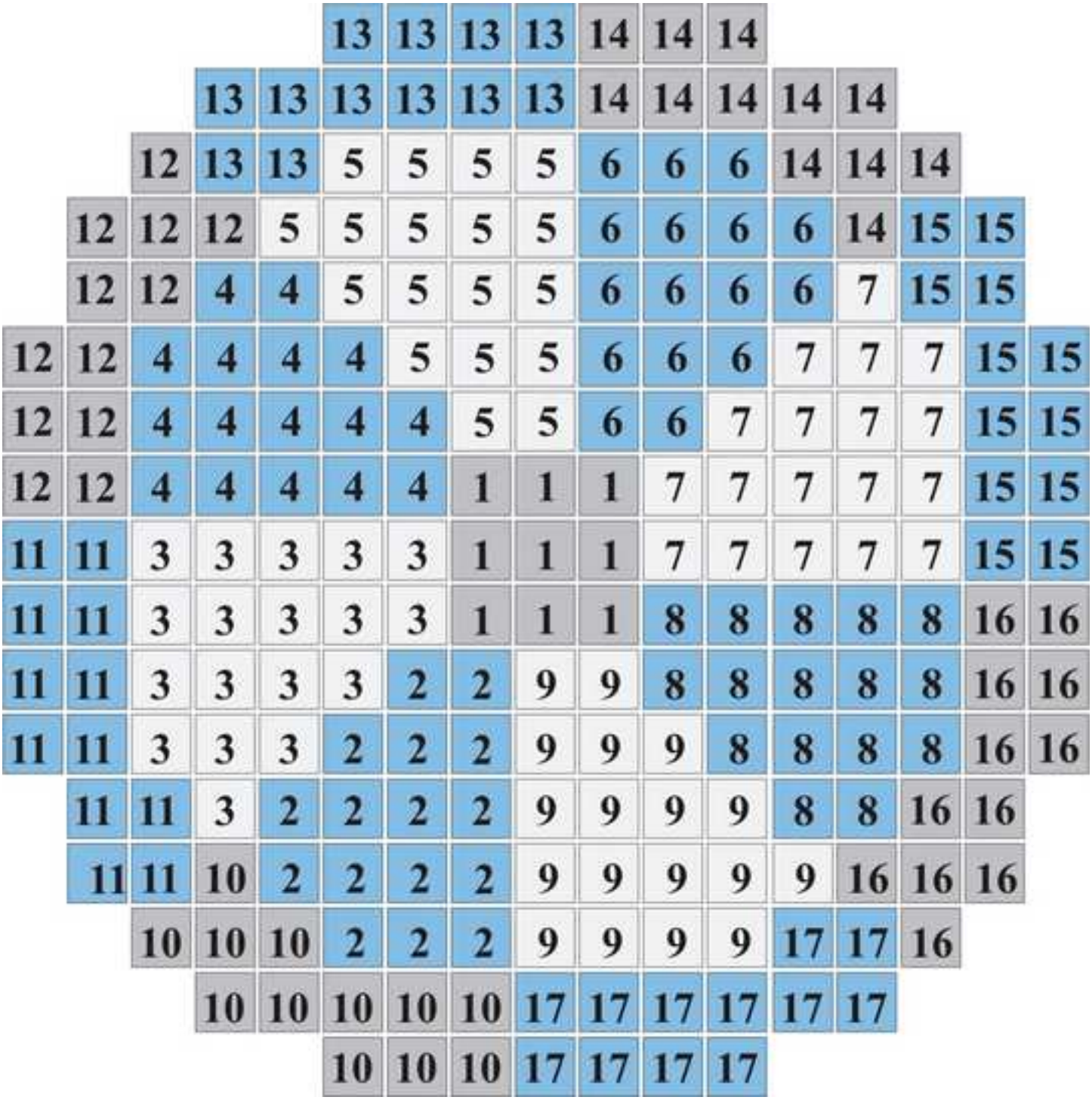

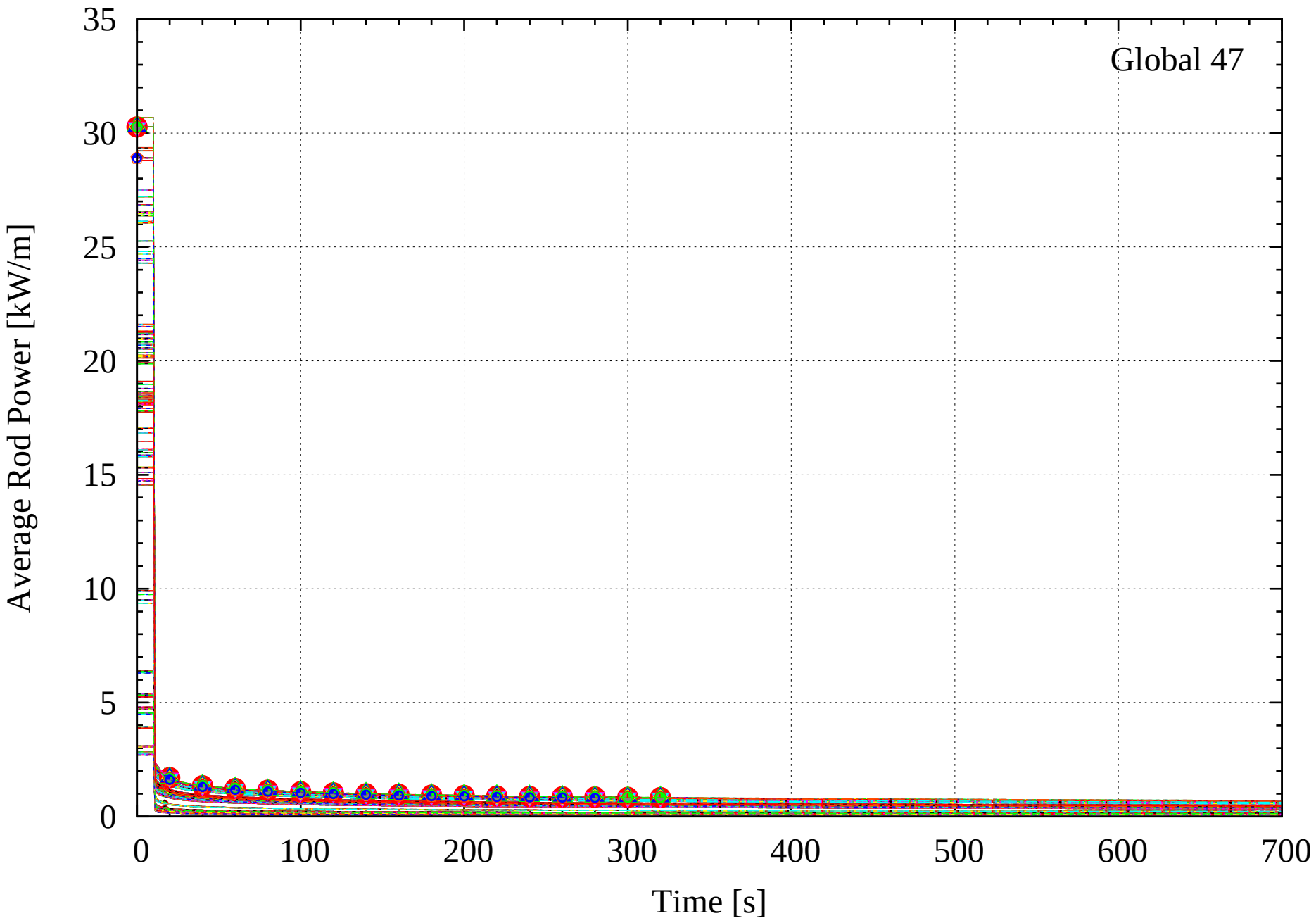
Global 47
Average Rod Power [kW/m]
Time [s]
0
5
10
15
20
25
30
35
0
100
200
300
400
500
600
700

Figure 4

Click here to download high resolution image

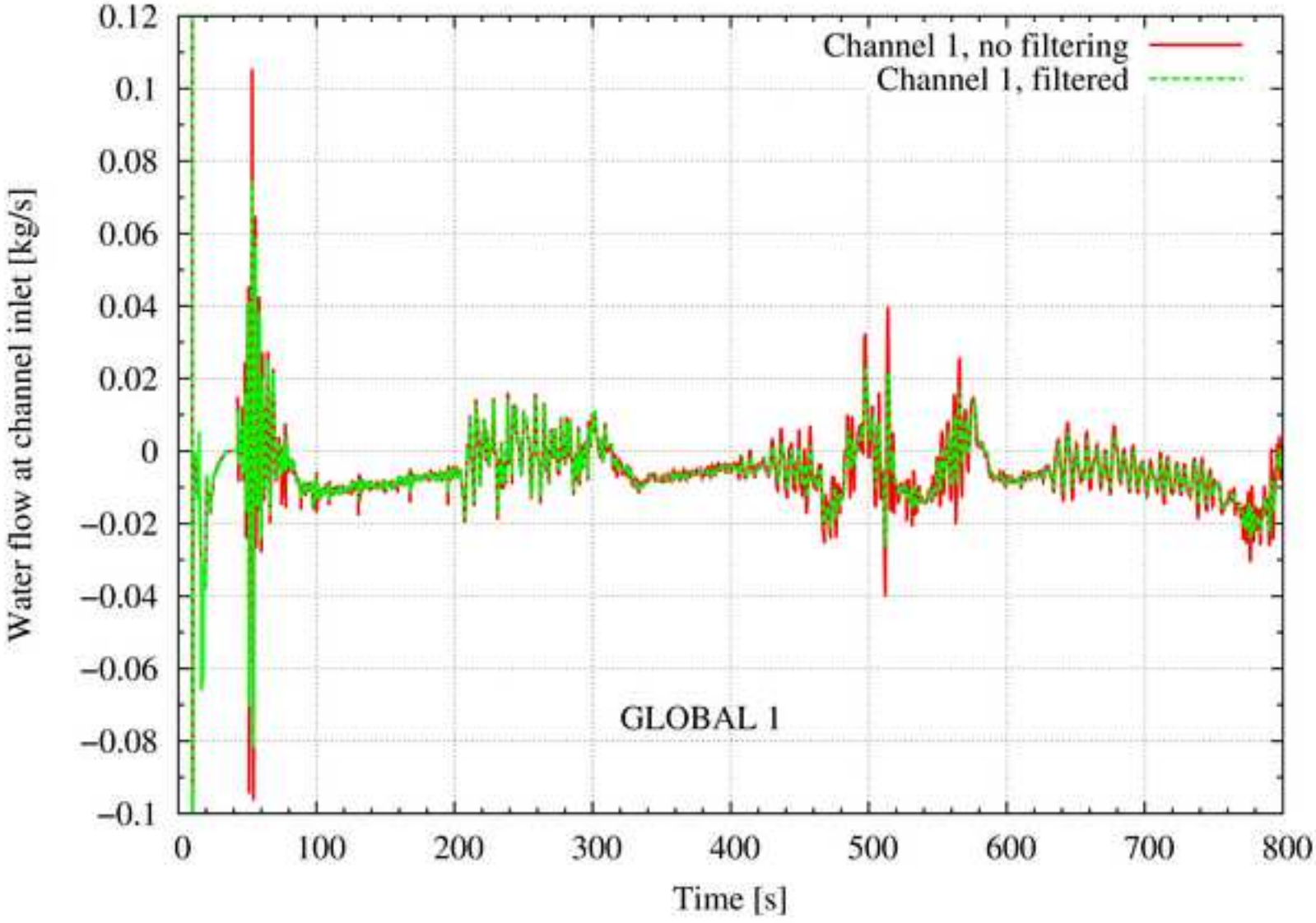

Figure 5

Click here to download high resolution image

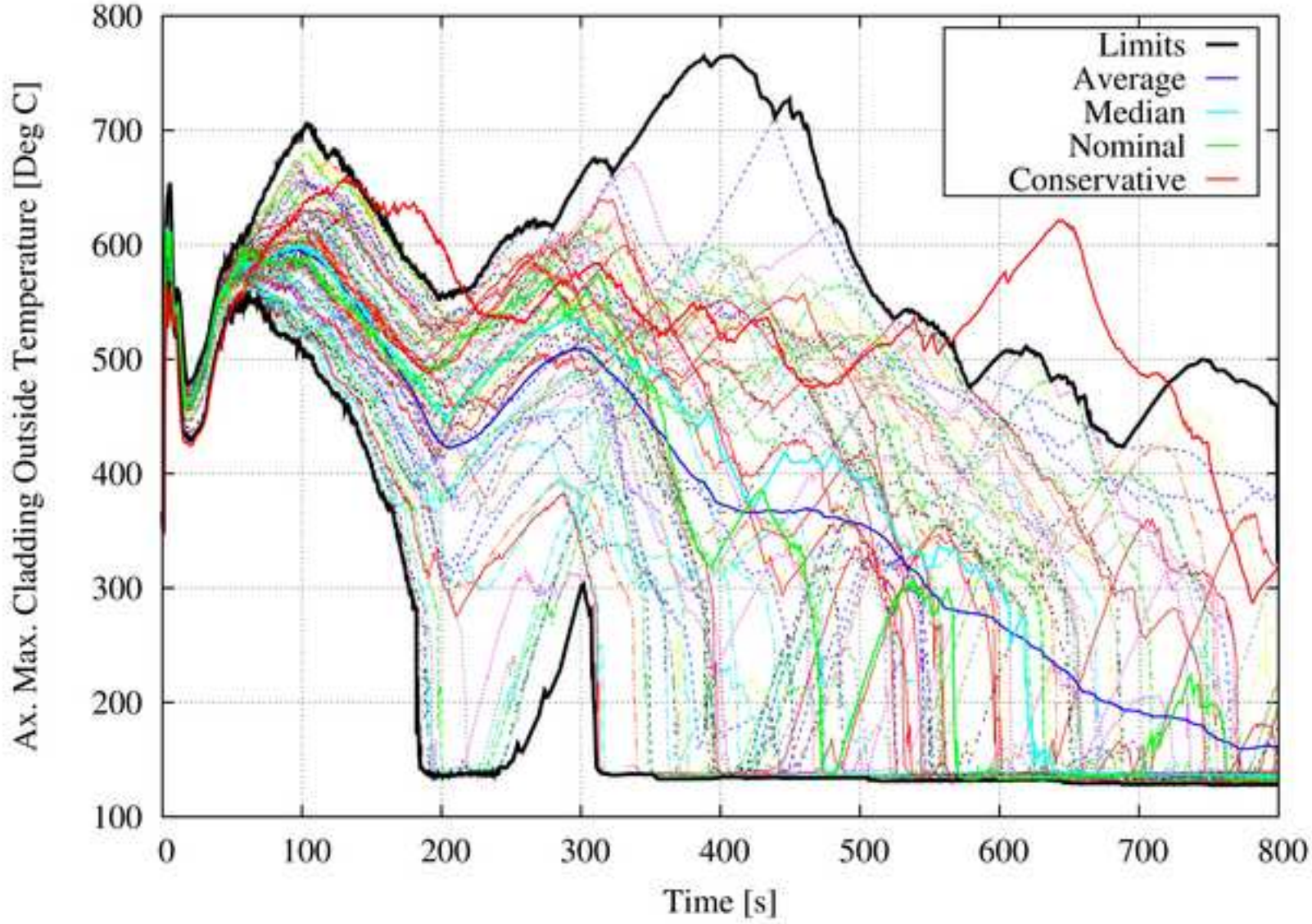

Figure 6

Click here to download high resolution image

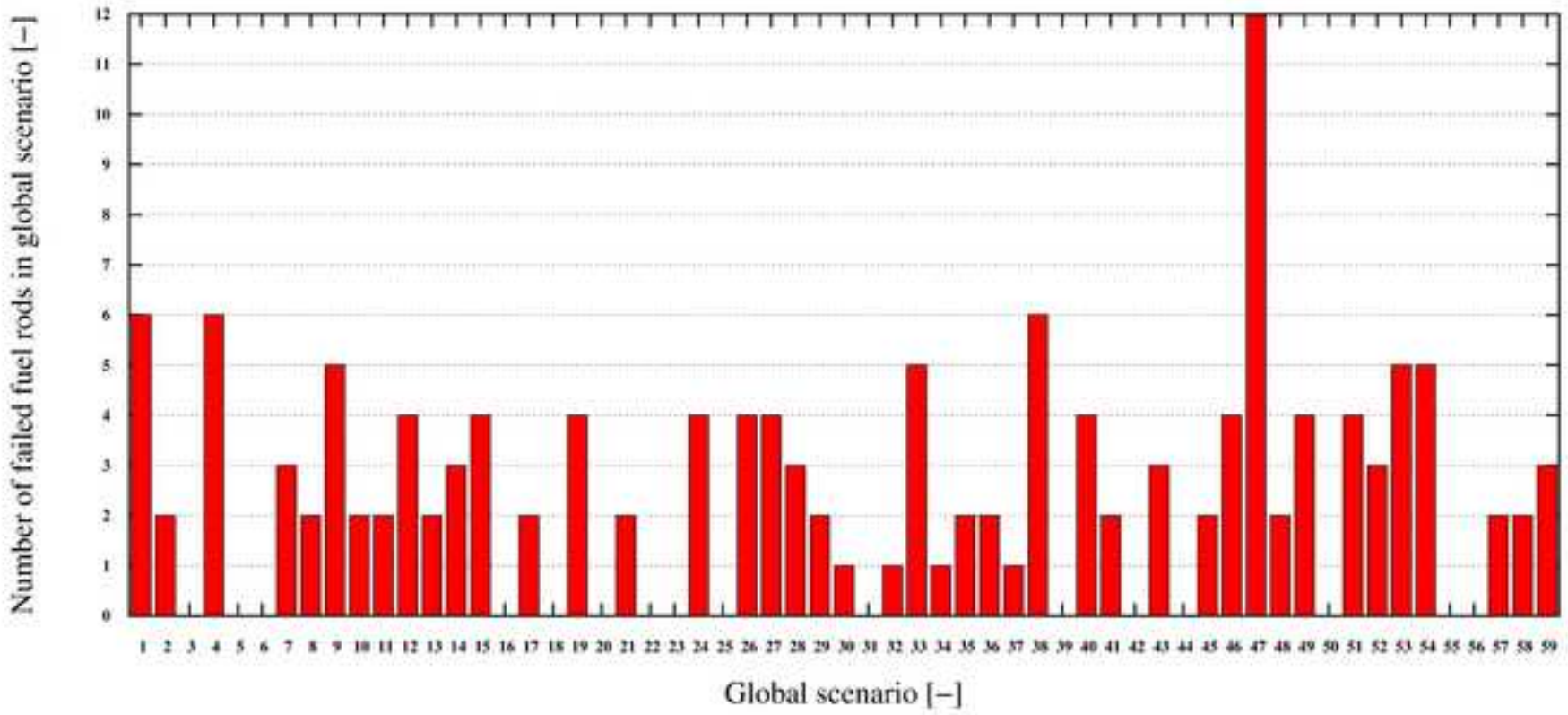

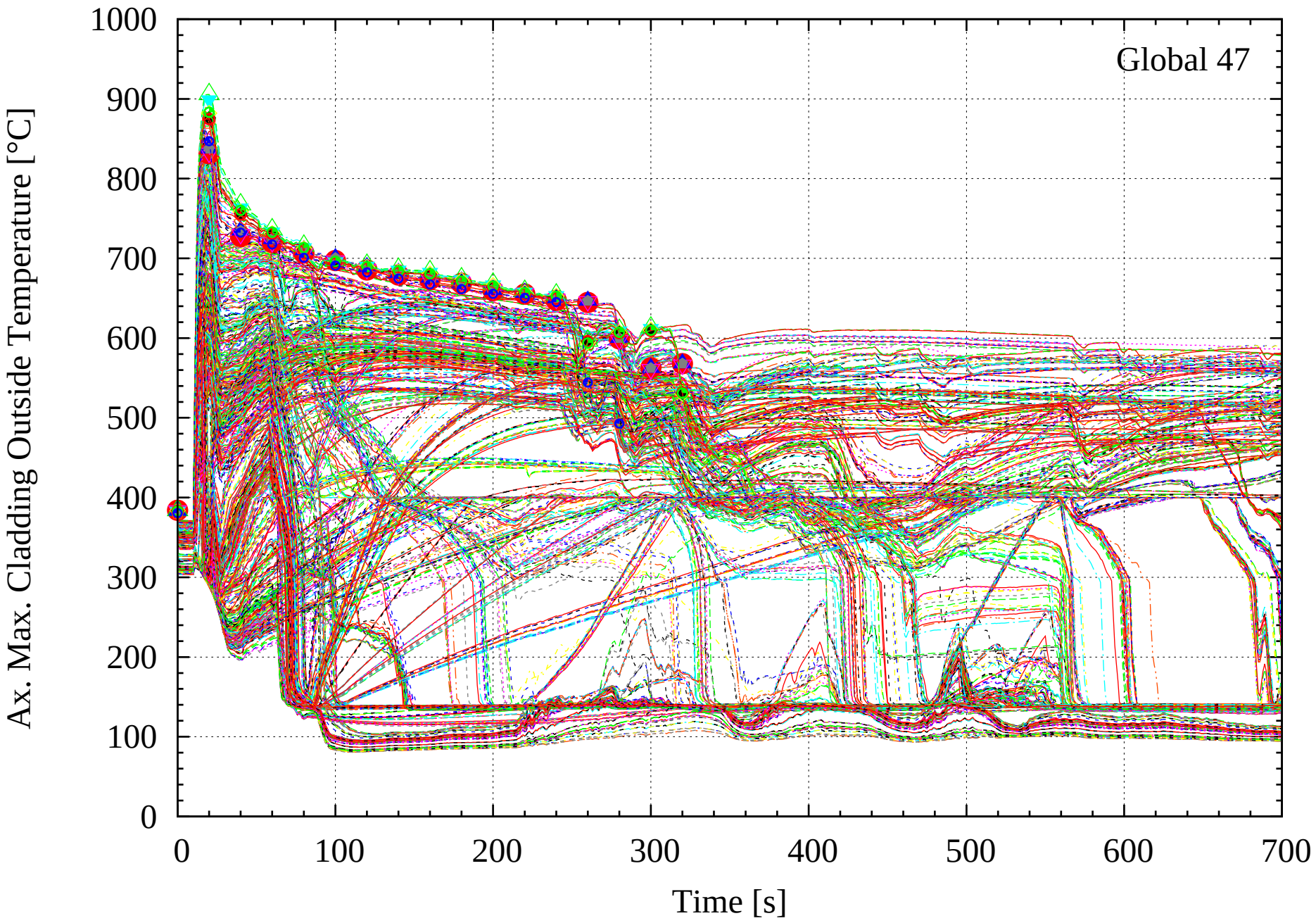
Global 47
Ax. Max. Cladding Outside Temperature [°C]
Time [s]
0
100
200
300
400
500
600
700
800
900
1000

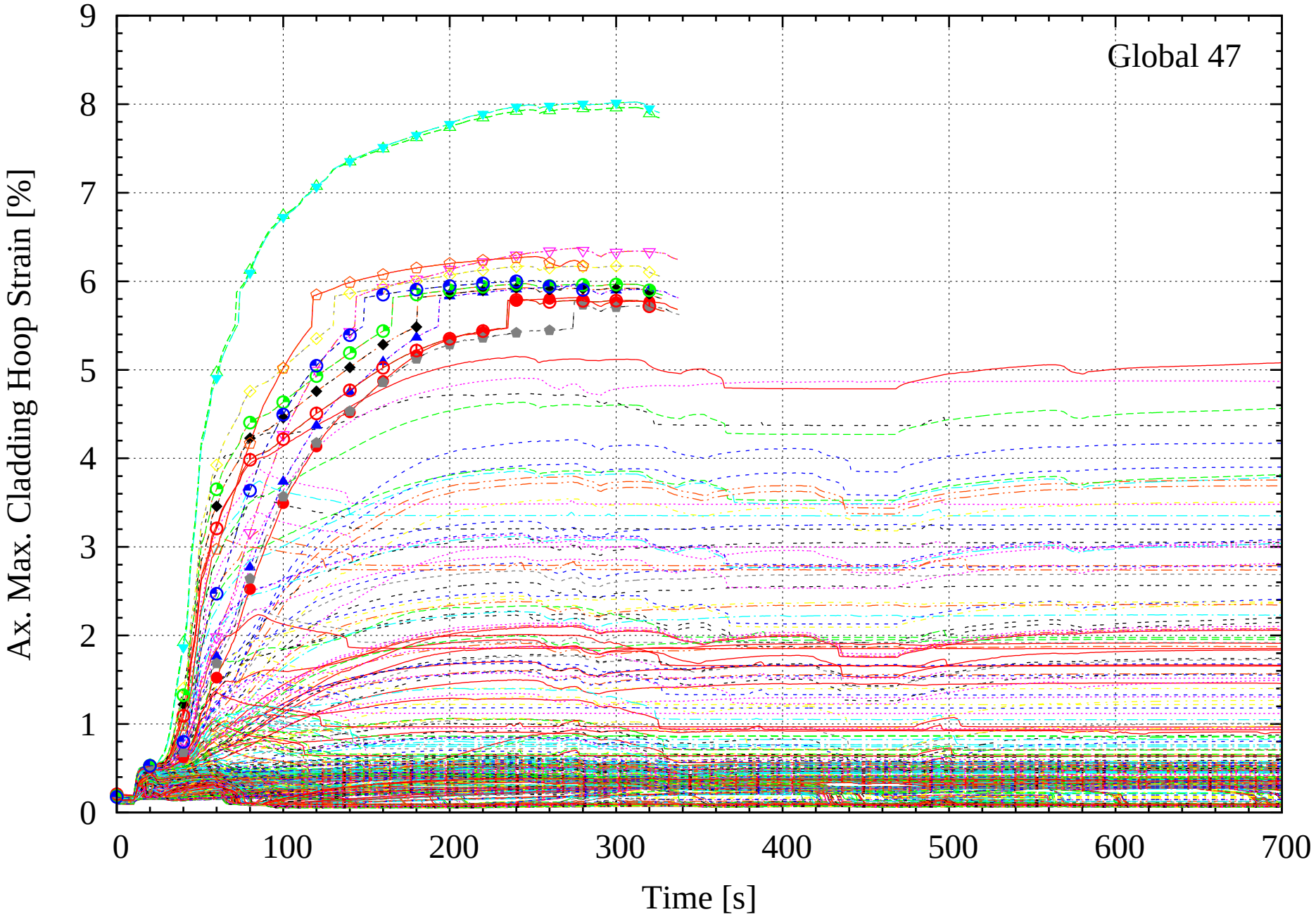
Global 47
Ax. Max. Cladding Hoop Strain [%]
Time [s]
0
1
2
3
4
5
6
7
8
9
0
100
200
300
400
500
600
700

Figure 9
Click here to download high resolution image

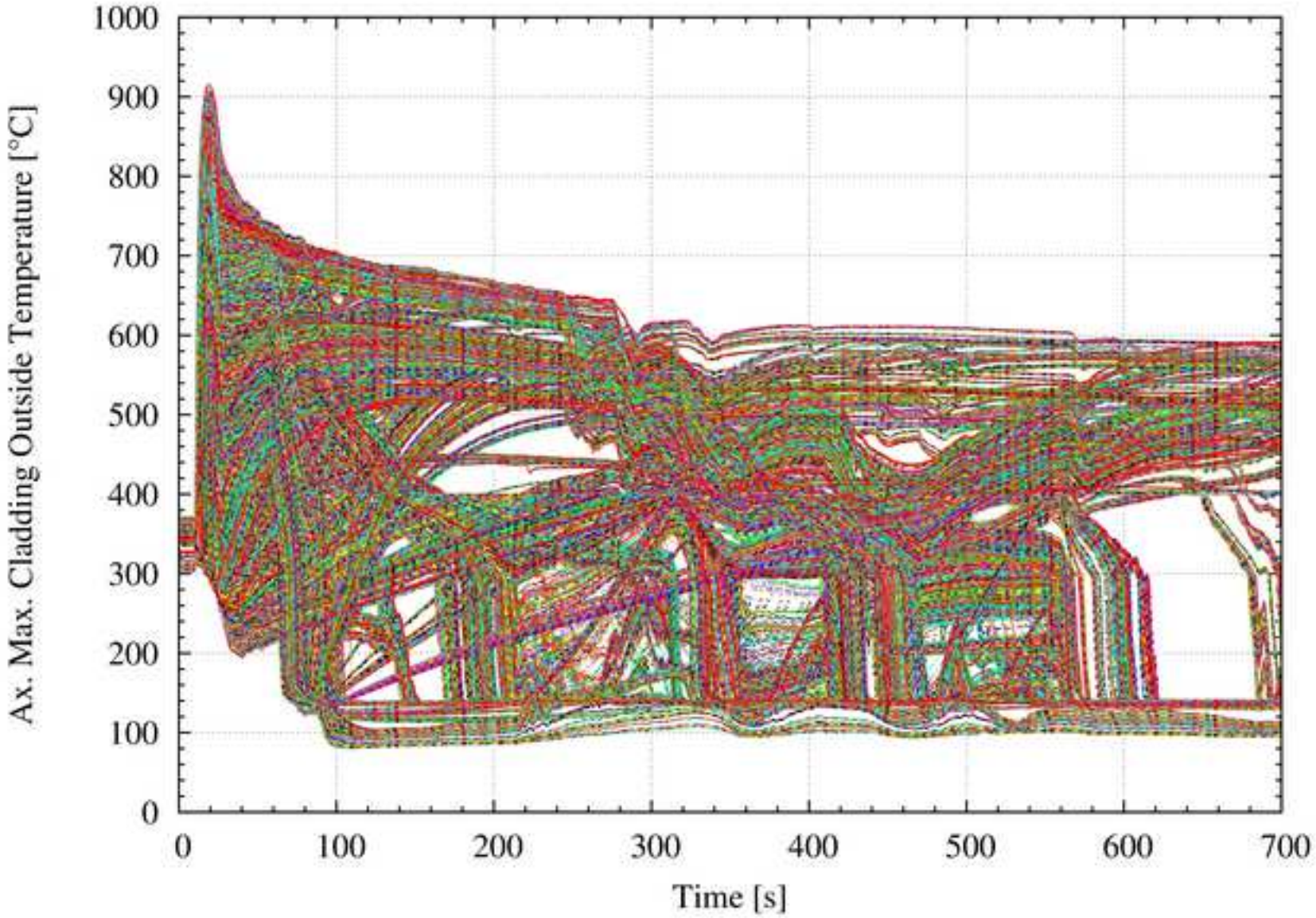

Figure 10

Click here to download high resolution image

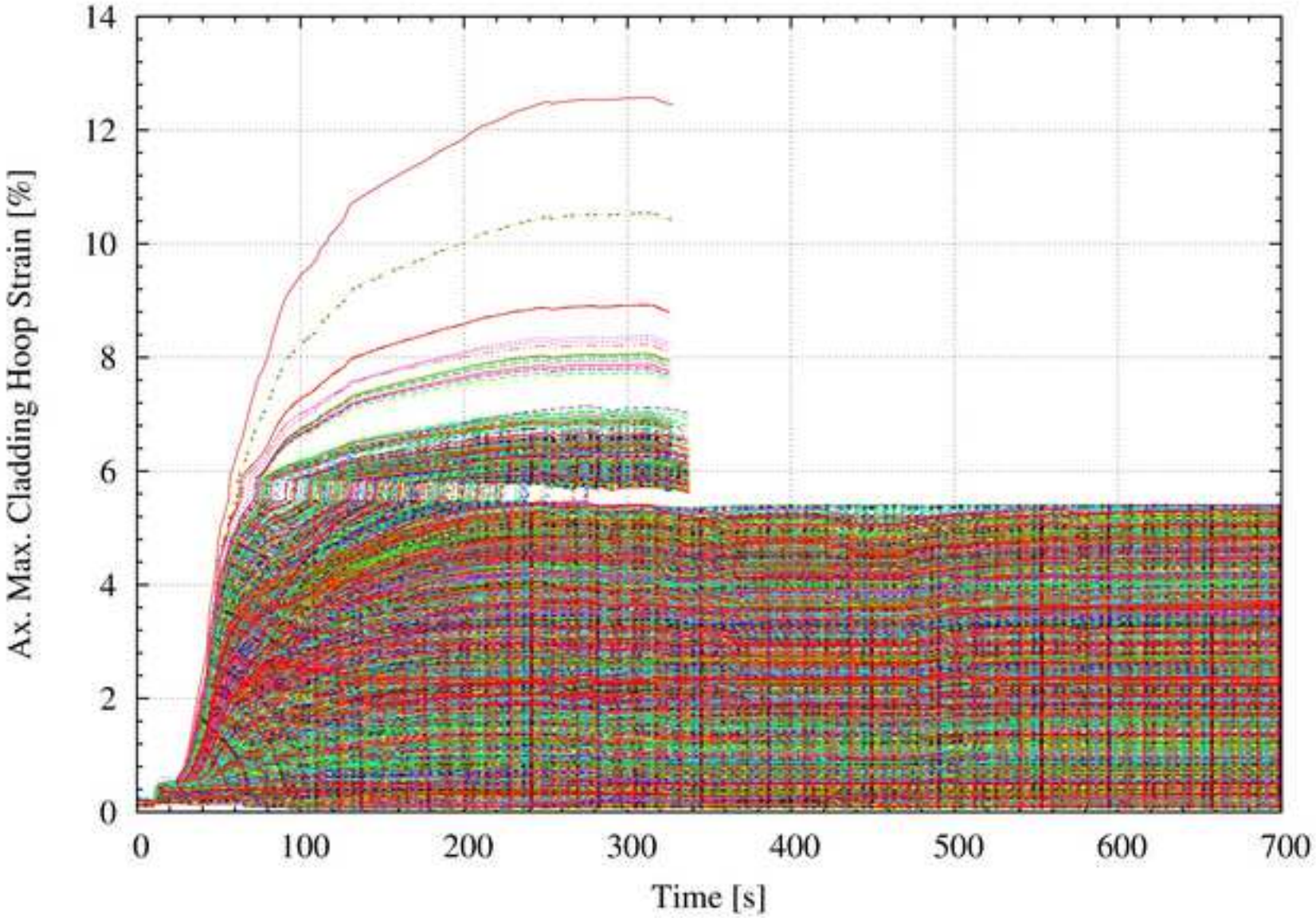

Figure 11

Click here to download high resolution image

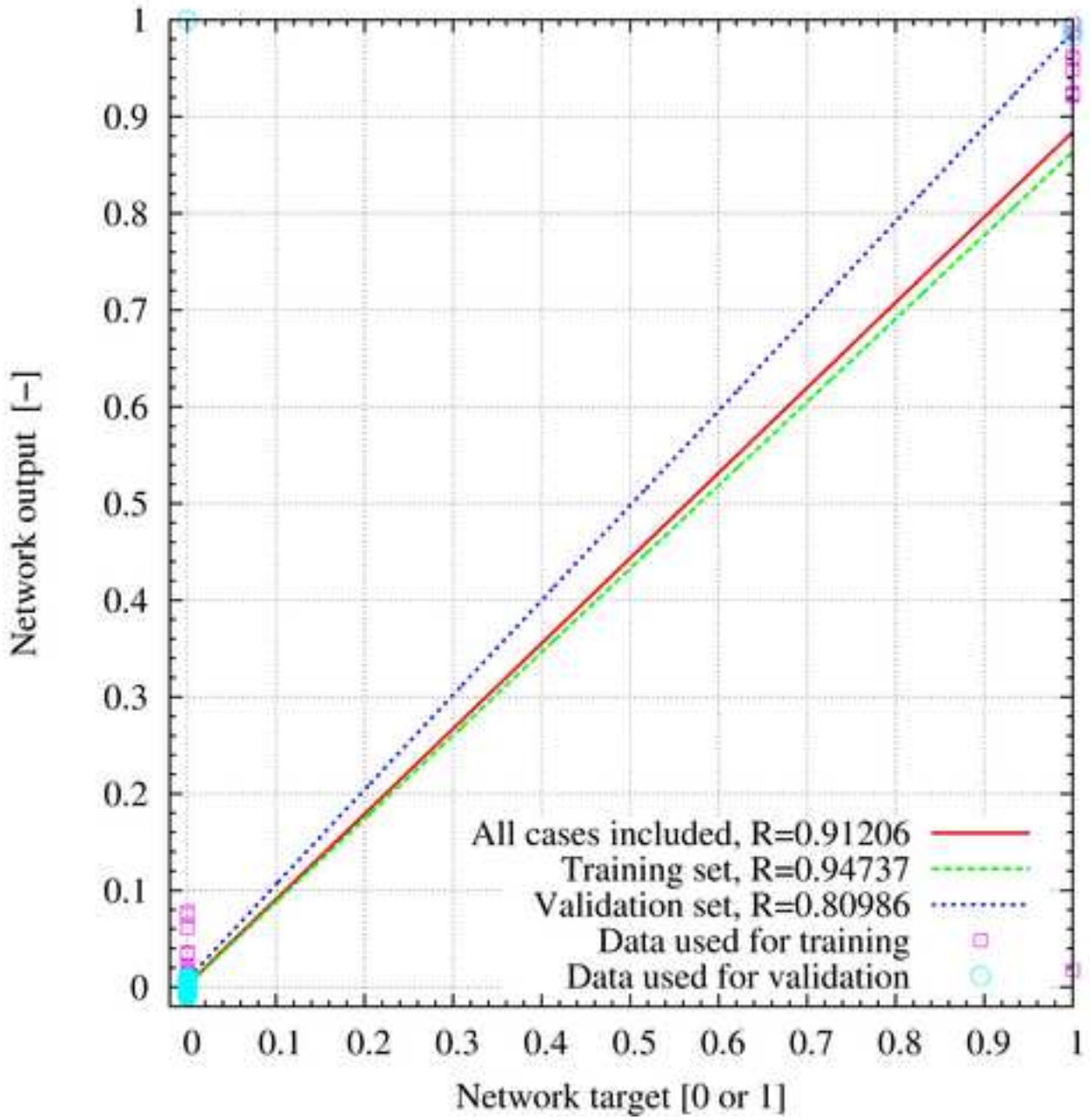

Figure 12
Click here to download high resolution image

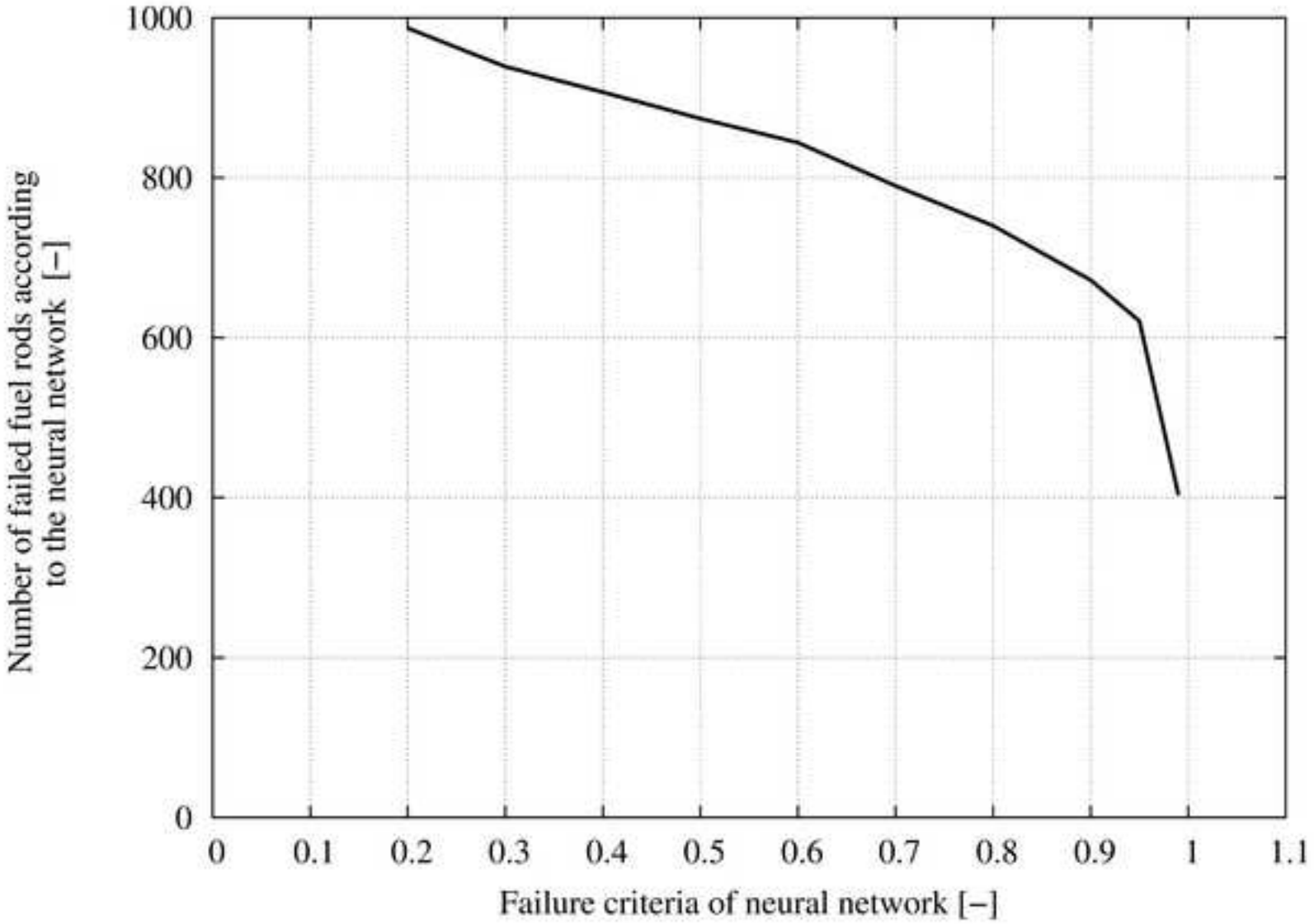

Figure 13

Click here to download high resolution image

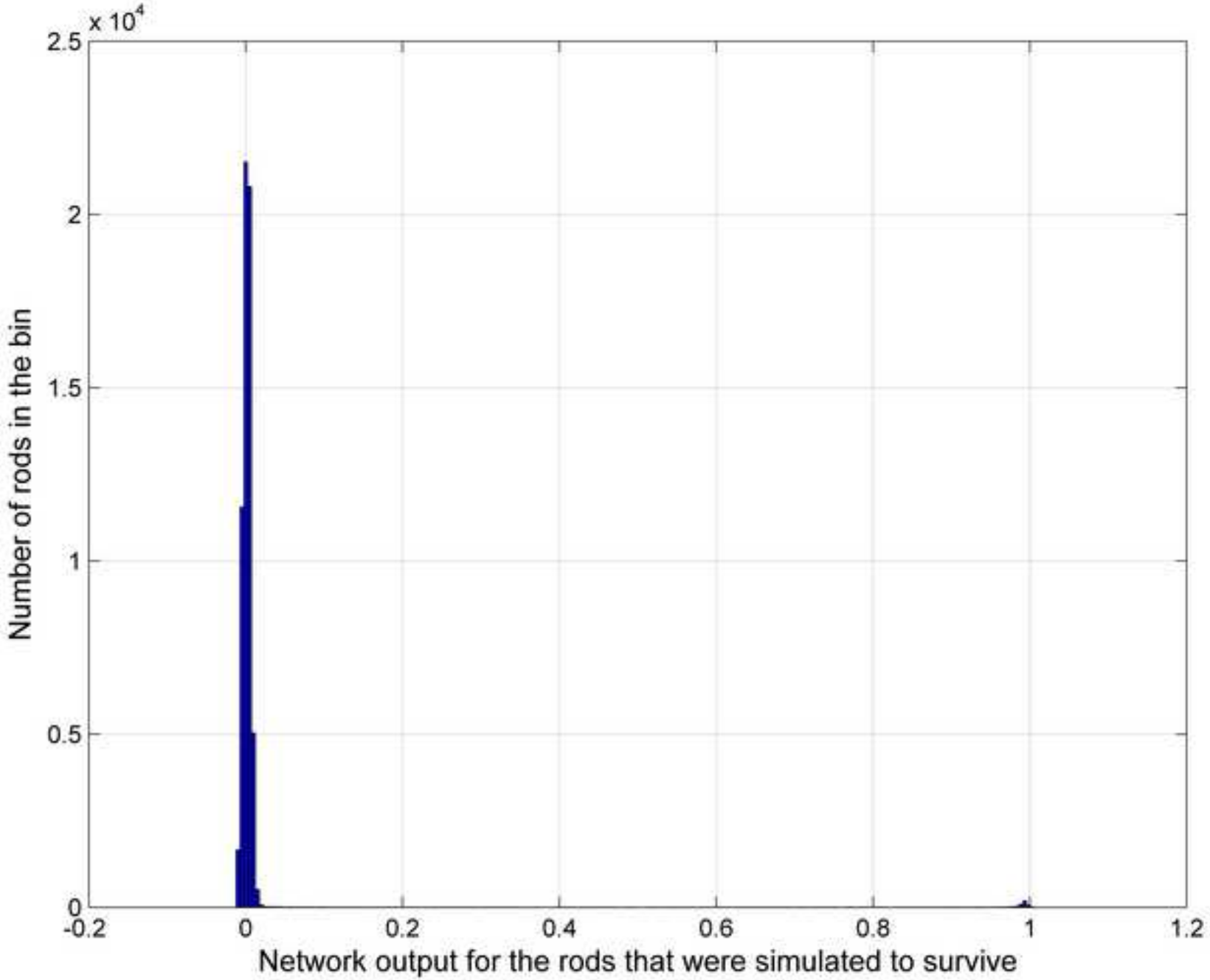

Figure 14

Click here to download high resolution image